Electronic Supplementary Material (ESI) for Chemical Society Reviews.

Main Group mechanochemistry: from curiosity to established protocols

Davin Tan[a] and Felipe García*[a]

[a] School of Physical and Mathematical Sciences, Division of Chemistry and Biological Chemistry, Nanyang Technological University, 21 Nanyang Link, Singapore 637371

1. Introduction and Background

1.1. Main group Mechanochemistry

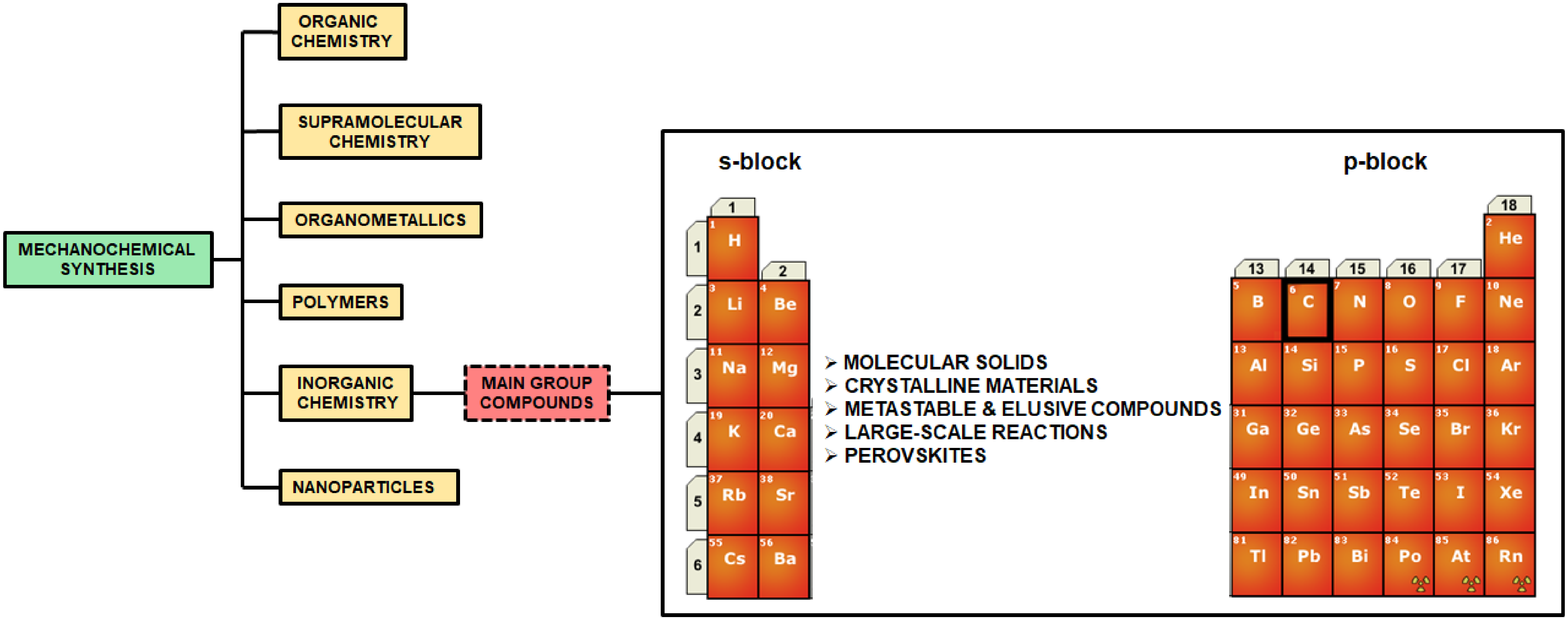

Figure 1. General overview of the field of mechanochemistry in organic synthesis, supramolecular synthesis, organometallics, nanoparticle synthesis, polymer synthesis and inorganic synthesis. The topic of main group mechanochemistry is highlighted in the orange box. All examples mentioned here are included and referenced in this review.

1.2 What is mechanochemistry?

Mechanochemical reaction is defined as: a chemical reaction that is induced by the direct absorption of mechanical energy. The mechanical energy can be imparted into the system by different modes of mechanical action (*i.e.*, impact, compression, shearing, stretching, grinding, *etc.*). This mechanical action can result in particle size reduction, creation of active sites for chemical reactivity – or the generation of fresh active surfaces – for other particles to contact, coalesce and react.

Key reference: A. D. McNaught and A. Wilkinson, IUPAC Compendium of Chemical Terminology, Blackwell Scientific Publications, Oxford, 1997

1.3 Overview and history of mechanochemistry

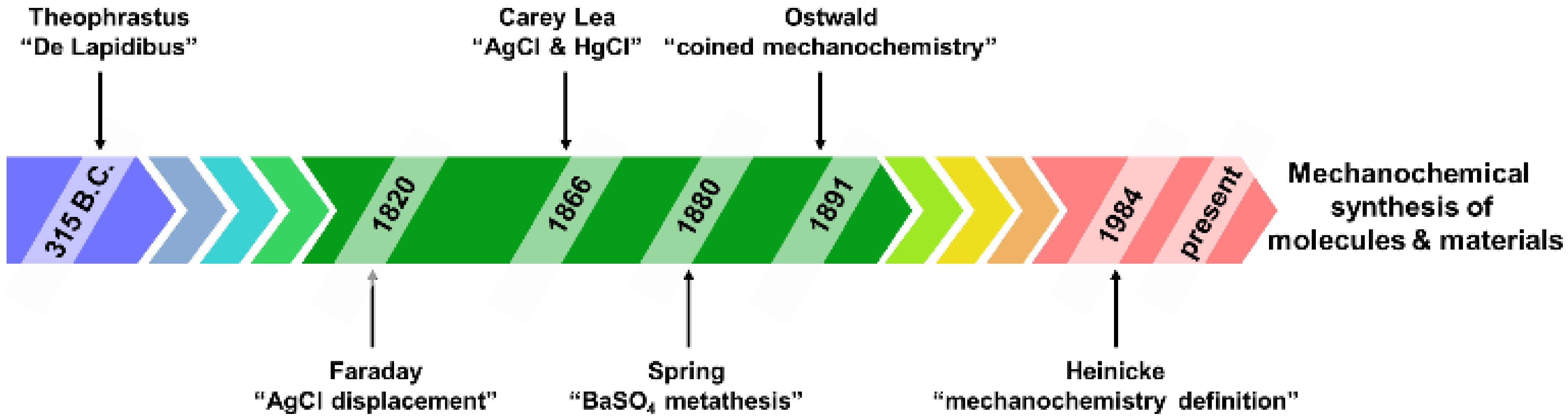

Figure 2. Chronological timeline of the historical development of mechanochemistry.

Key reference: L. Takacs, Chem. Soc. Rev., 2013, 42, 7649-7659 and references therein

1.4 Tools, symbols and techniques

1.4.1 Mechanochemical nomenclature

Scheme 2. Symbolic representation of (a) solvothermal, (b) sonochemical, (c) microwave irradiation, (d) photochemical and (e) mechanochemical reactions.

Key references:

S. L. James, C. J. Adams, C. Bolm, D. Braga, P. Collier, T. Friščić, F. Grepioni, K. D. M. Harris, G. Hyett, W. Jones, A. Krebs, J. Mack, L. Maini, A. G. Orpen, I. P. Parkin, W. C. Shearouse, J. W. Steed, and D. C. Waddell, Chem. Soc. Rev., 2012, 41, 413-447 and references therein.

J. Andersen and J. Mack. Green Chem., 2018, 20, 1435-1443 and references therein.

N. R. Rightmire and T. P. Hanusa, Dalton Trans., 2016, 45, 2352-2362 and references therein

1.4 Tools, symbols and techniques

1.4.2 Mechanochemical tools and instruments

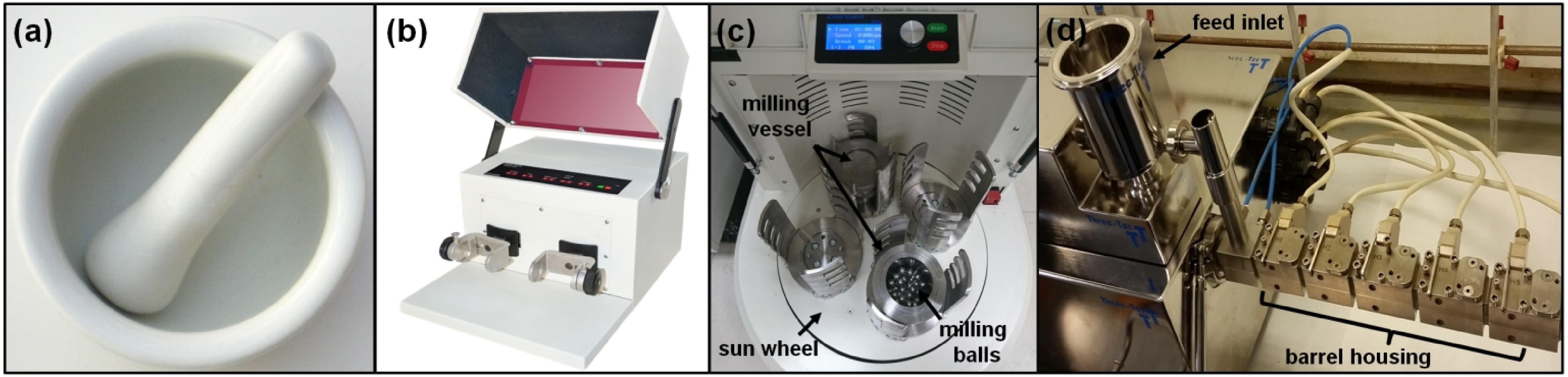

Figure 3. Pictures of (a) mortar and pestle, (b) electric shaker mill, (c) planetary mill and (d) twin-screw extruder. Reproduced with permission from reference.

Key reference:

L. Takacs, Chem. Soc. Rev., 2013, 42, 7649-7659 and references therein

J. Andersen and J. Mack. Green Chem., 2018, 20, 1435-1443 and references therein.

1.4 Tools, symbols and techniques

1.4.2 Mechanochemical tools and instruments

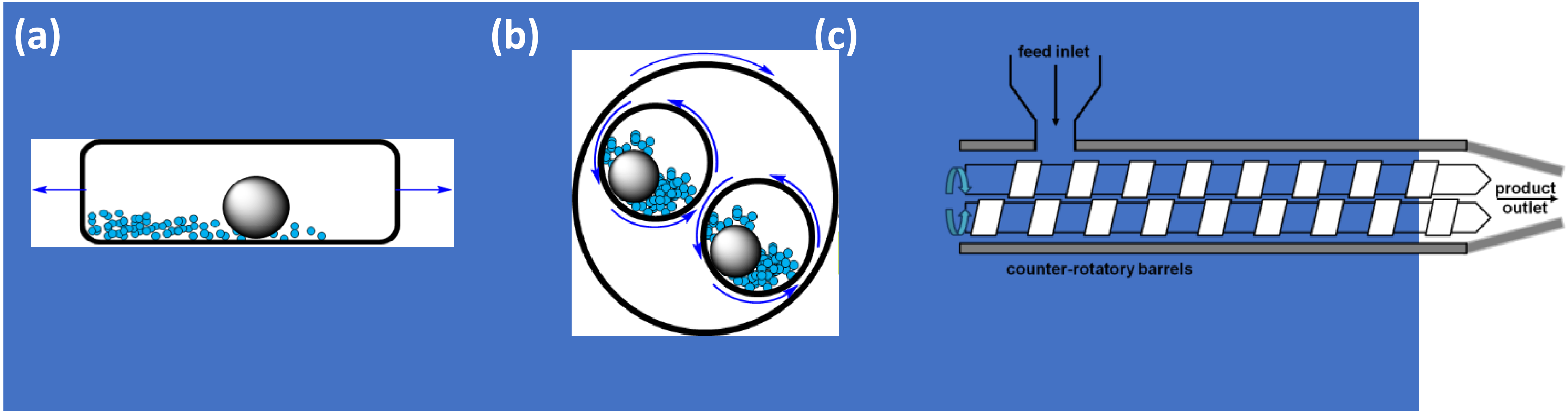

Figure 4. Schematic representation illustrating the mode of motion of the cross-section of a (a) shaker and (b) planetary mill, and (c) twin-screw extruder.

Key reference:

S. L. James, C. J. Adams, C. Bolm, D. Braga, P. Collier, T. Friščić, F. Grepioni, K. D. M. Harris, G. Hyett, W. Jones, A. Krebs, J. Mack, L. Maini, A. G. Orpen, I. P. Parkin, W. C. Shearouse, J. W. Steed, and D. C. Waddell, Chem. Soc. Rev., 2012, 41, 413-447 and references therein

J. Andersen and J. Mack. Green Chem., 2018, 20, 1435-1443 and references therein.

1.4 Tools, symbols and techniques

1.4.2 Mechanochemical tools and instruments

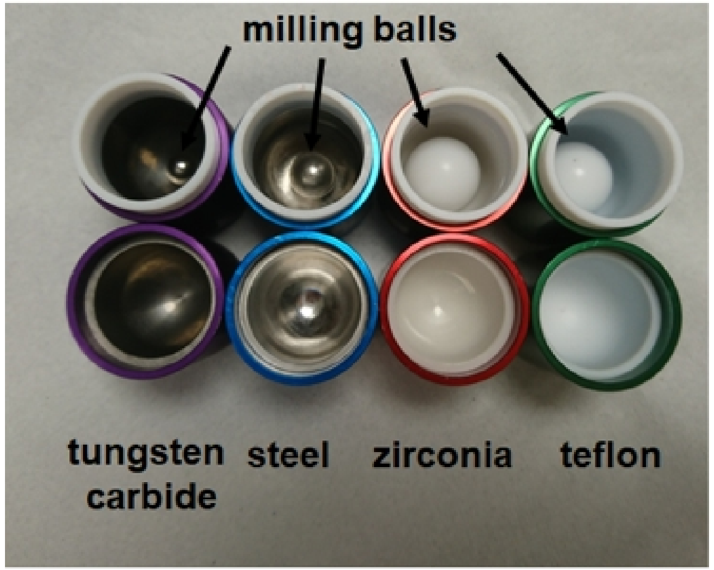

Figure 5. Milling media jars and balls. Reproduced with permission from FormTech Scientific.

Key reference:

S. L. James, C. J. Adams, C. Bolm, D. Braga, P. Collier, T. Friščić, F. Grepioni, K. D. M. Harris, G. Hyett, W. Jones, A. Krebs, J. Mack, L. Maini, A. G. Orpen, I. P. Parkin, W. C. Shearouse, J. W. Steed, and D. C. Waddell, Chem. Soc. Rev., 2012, 41, 413-447 and references therein

J. Andersen and J. Mack. Green Chem., 2018, 20, 1435-1443 and references therein.

1.4 Tools, symbols and techniques

1.4.4 Liquid-assisted grinding (LAG) and milling auxiliaries

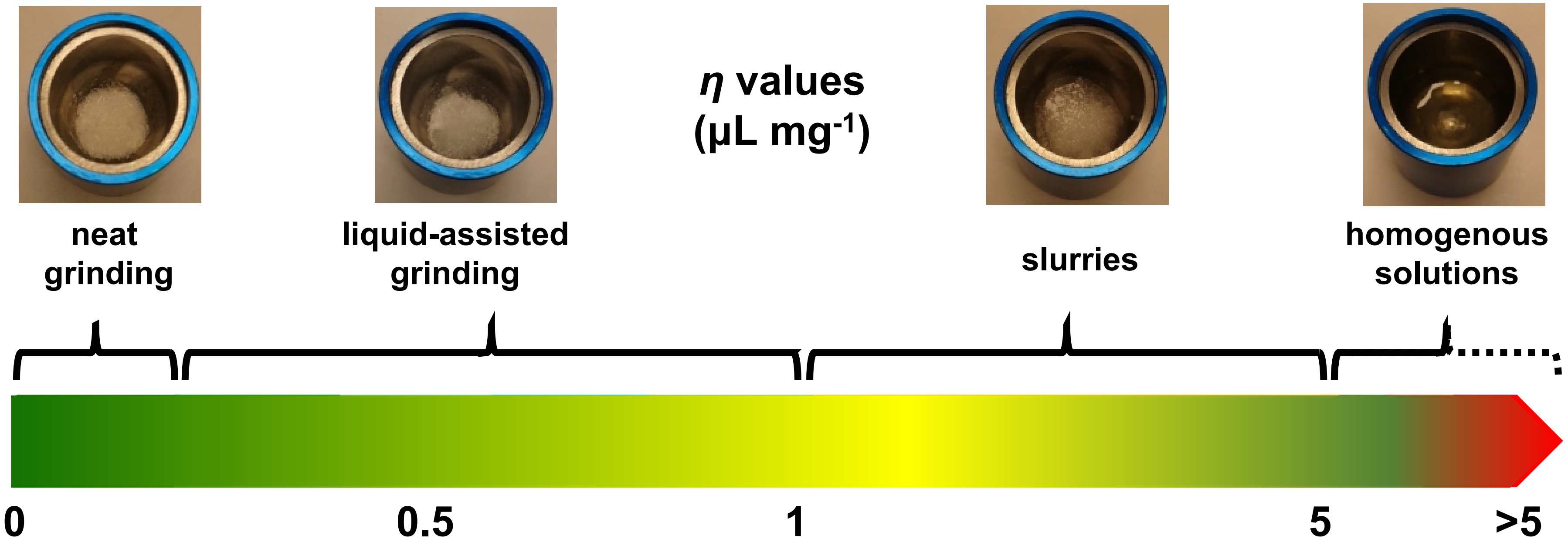

Figure 6. Range of **η** values and appearance of the reagents.

Key reference:

D. Tan, L. Loots and T. Friščić, *ChemComm.*, **2016**, *52*, 7760 and references therein..

1.4 Tools, symbols and techniques

1.4.5 Solution *vs* mechanochemical methods

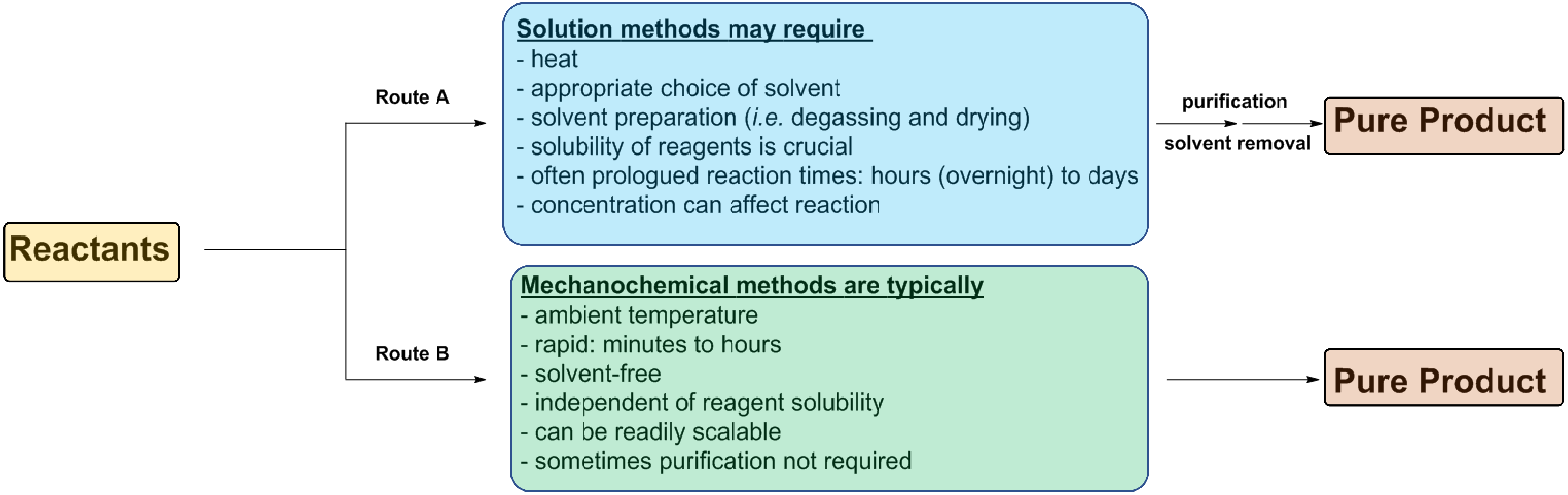

Reactants

Route A

Solution methods may require
- heat
- appropriate choice of solvent
- solvent preparation (*i.e.* degassing and drying)
- solubility of reagents is crucial
- often prologued reaction times: hours (overnight) to days
- concentration can affect reaction

purification

solvent removal

Pure Product

Route B

Mechanochemical methods are typically
- ambient temperature
- rapid: minutes to hours
- solvent-free
- independent of reagent solubility
- can be readily scalable
- sometimes purification not required

Pure Product

Scheme 3. Variables associated with solvent-based and mechanochemical methodologies *via* **Route A** and **Route B**, respectively.

Key references:

N. R. Rightmire and T. P. Hanusa, *Dalton Trans.*, **2016**, *45*, 2352-2362 and references therein.

A. A. Geciauskaite and F. García, Beilstein J. Org. Chem. 2017, 13, 2068-2077 and references therein.

1.4 Tools, symbols and techniques

1.4.6 Mechanochemical reactions mechanisms: In situ vs. Ex situ monitoring.

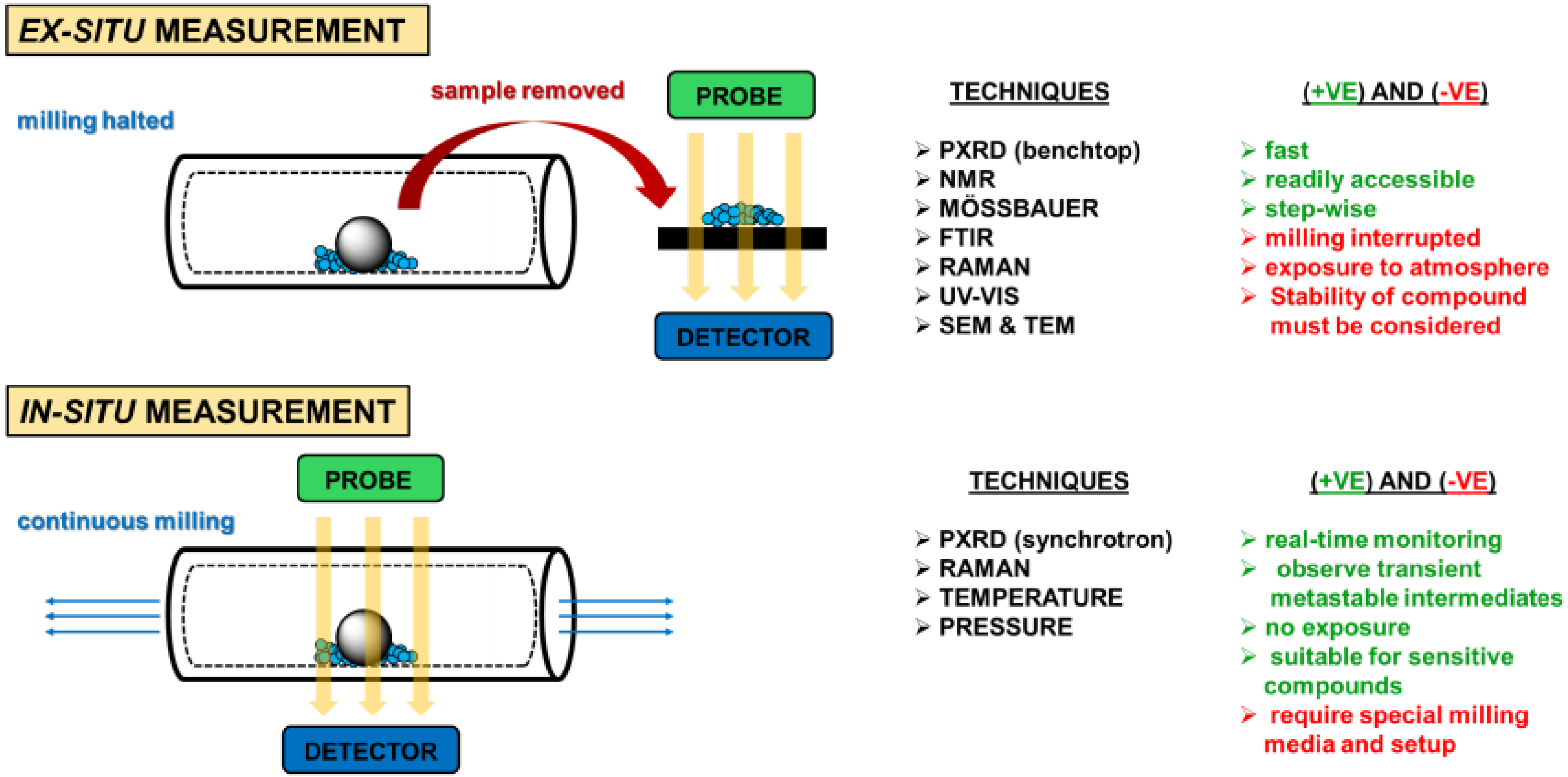

TECHNIQUES

- PXRD (benchtop)
- NMR
- MÖSSBAUER
- FTIR
- RAMAN
- UV-VIS
- SEM & TEM

(+VE) AND (-VE)

- fast
- readily accessible
- step-wise
- milling interrupted
- exposure to atmosphere
- Stability of compound must be considered

TECHNIQUES

- PXRD (synchrotron)
- RAMAN
- TEMPERATURE
- PRESSURE

(+VE) AND (-VE)

- real-time monitoring
- observe transient metastable intermediates
- no exposure
- suitable for sensitive compounds
- require special milling media and setup

Figure 7. Comparison of *ex situ* and *in situ* characterization techniques for mechanochemical reactions

Key reference:

K. Užarević, I. Halasz, and T. FriščićJ. Phys. Chem. Lett., 2015, 6, 4129 and references therein.

2. From Molecules to Materials: s-block

2.1 Molecular species of the s-block

2.1.1 Group 1: Hydrides and alkaline metals

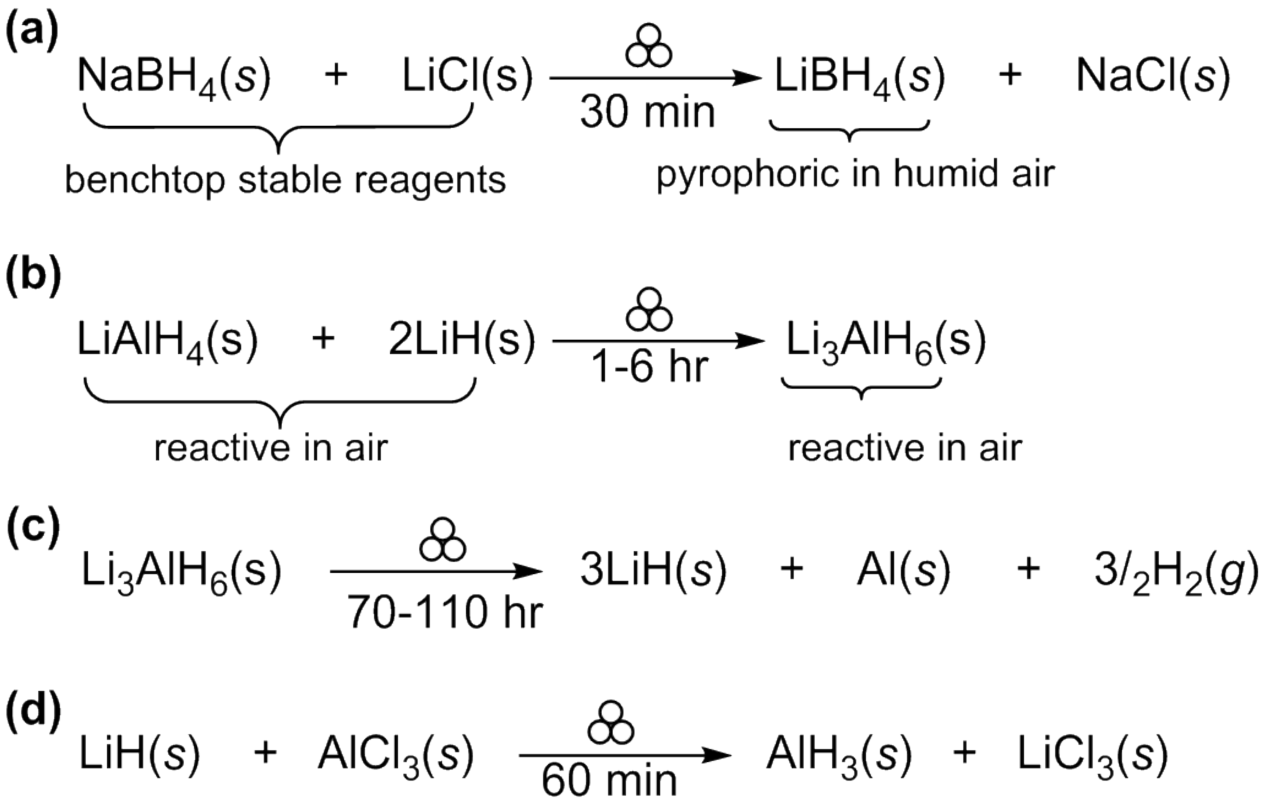

Scheme 4. (a) Formation of reactive $LiBH_4$ from $NaBH_4$ and LiCl, (b) solid-state synthesis of the alane Li_3AlH_6 from $LiAlH_4$ and LiH, (c) degradation and release of H_2 gas by prolonged milling of Li_3AlH_6, (d) formation of AlH_3 by salt metathesis of LiH and $AlCl_3$.

2.1 Molecular species of the s-block

2.1.2 Group 2: Alkaline-earth metals

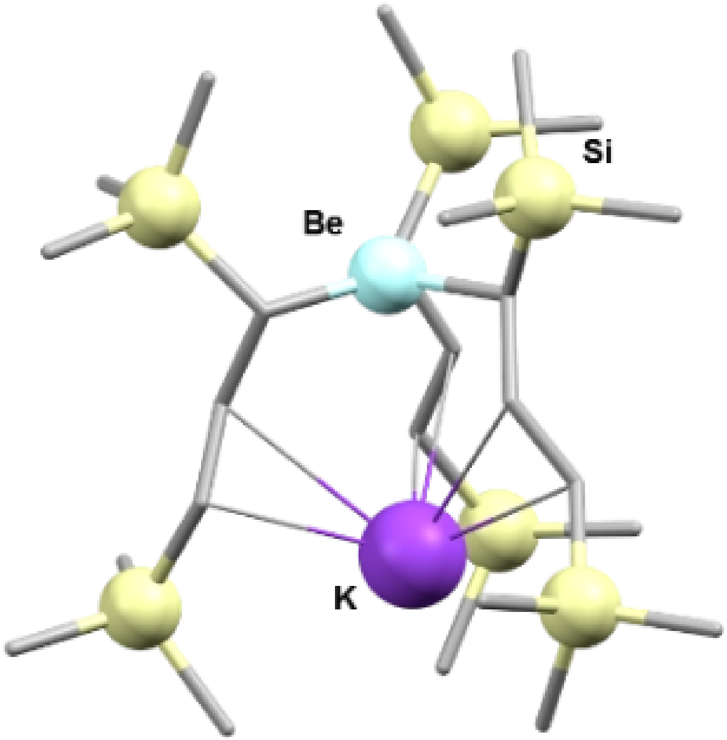

Figure 8. Molecular structure of the potassium tris-bis(trimethylsilyl)propyl-beryllate as determined by X-ray diffraction crystallography. Hydrogen atoms are omitted for clarity.

2.1 Molecular species of the s-block

2.1.2 Group 2: Alkaline-earth metals

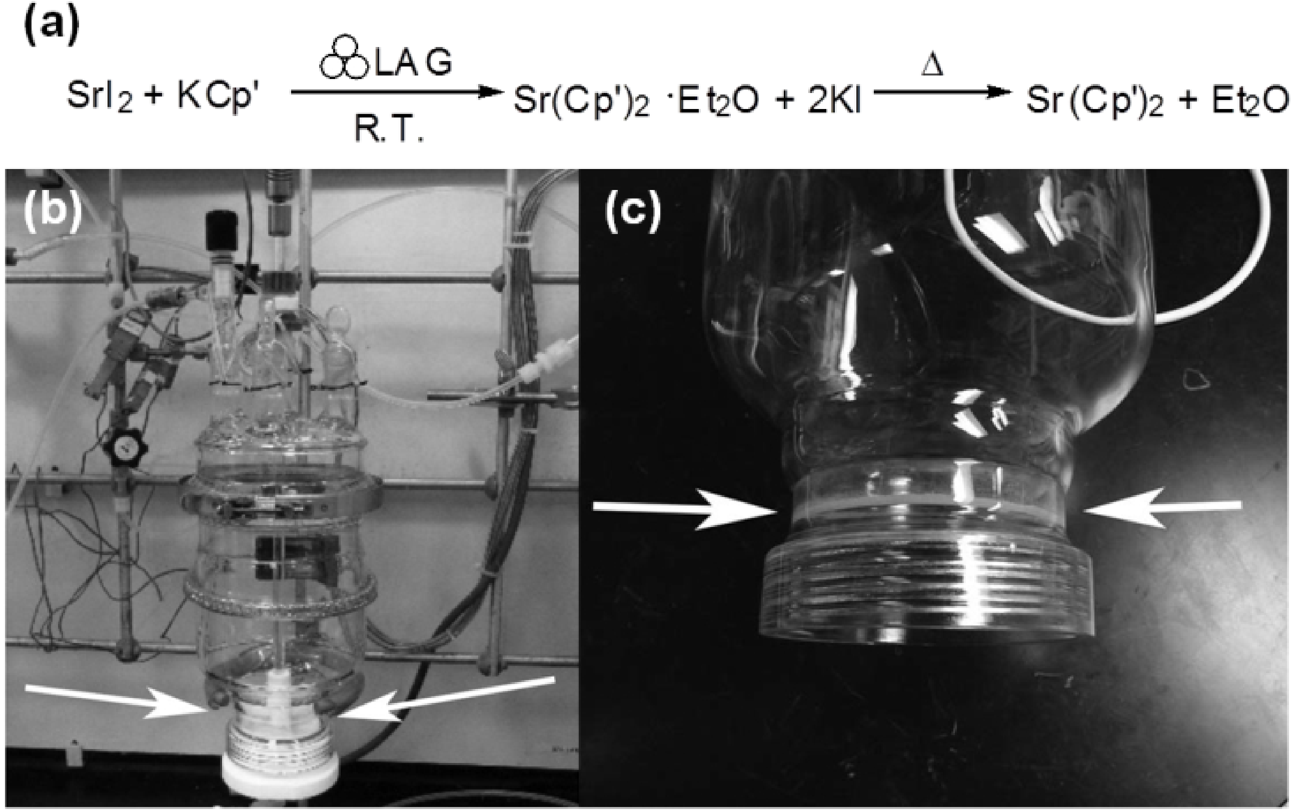

Figure 9. (a) Synthesis of the Sr(Cp’)$_2$ organometallic complex by LAG and thermal removal of the Et$_2$O solvate. (b) Picture of the custom mechanochemical reactor assembly is based on commercially available large-scale glassware. (c) The arrows show gradual wear and tear from the milling media on the sides of the glass reactor, yet no metal contaminants were found in the product. Reproduced with permission from reference 27.

2.2 Materials containing s-block elementsecular species of the s-block

2.2.1 Group 1: Hydrides and alkaline metals

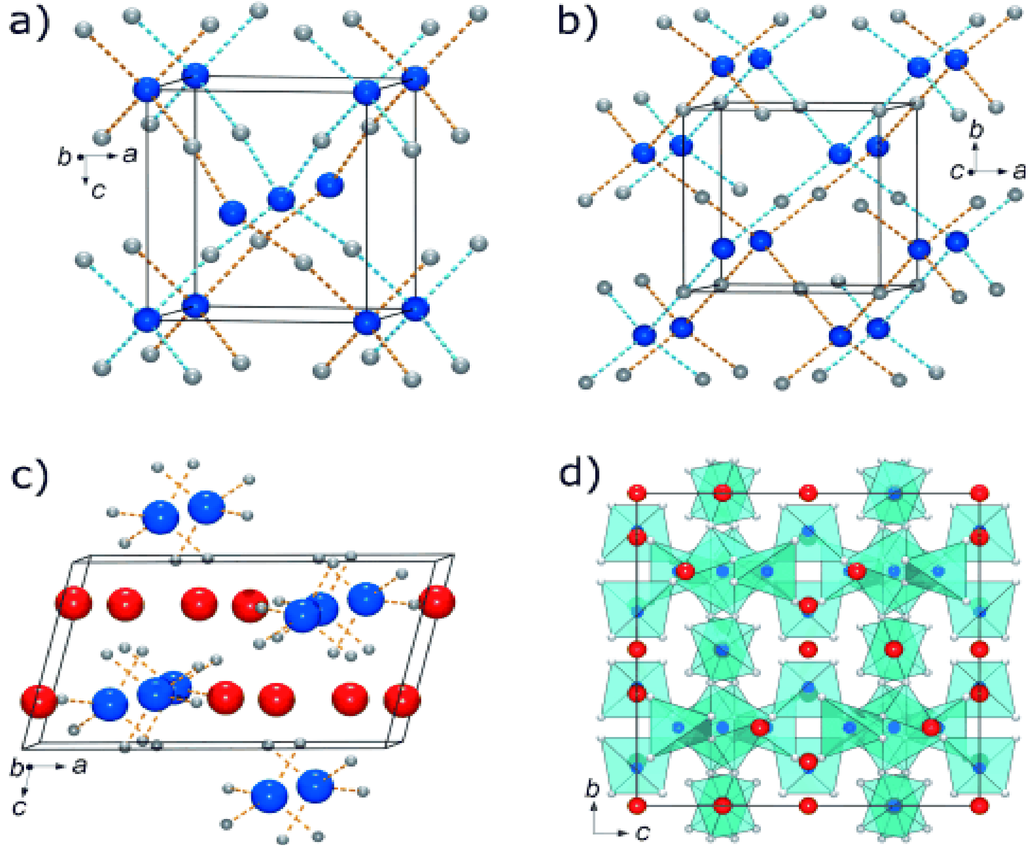

Figure 10. Crystal structures of (a) α-$Cd(BH_4)_2$, (b) β-$Cd(BH_4)_2$, (c) K_2Cd-$(BH_4)_4$, and (d) $KCd(BH_4)_3$. Hydrogen atoms are omitted for clarity. The following colouring scheme is used : Cd (blue), K (red), B (light grey). Reproduced with permission from reference 28.

2.2 Materials containing s-block elementsecular species of the s-block

2.2.1 Group 1: Hydrides and alkaline metals

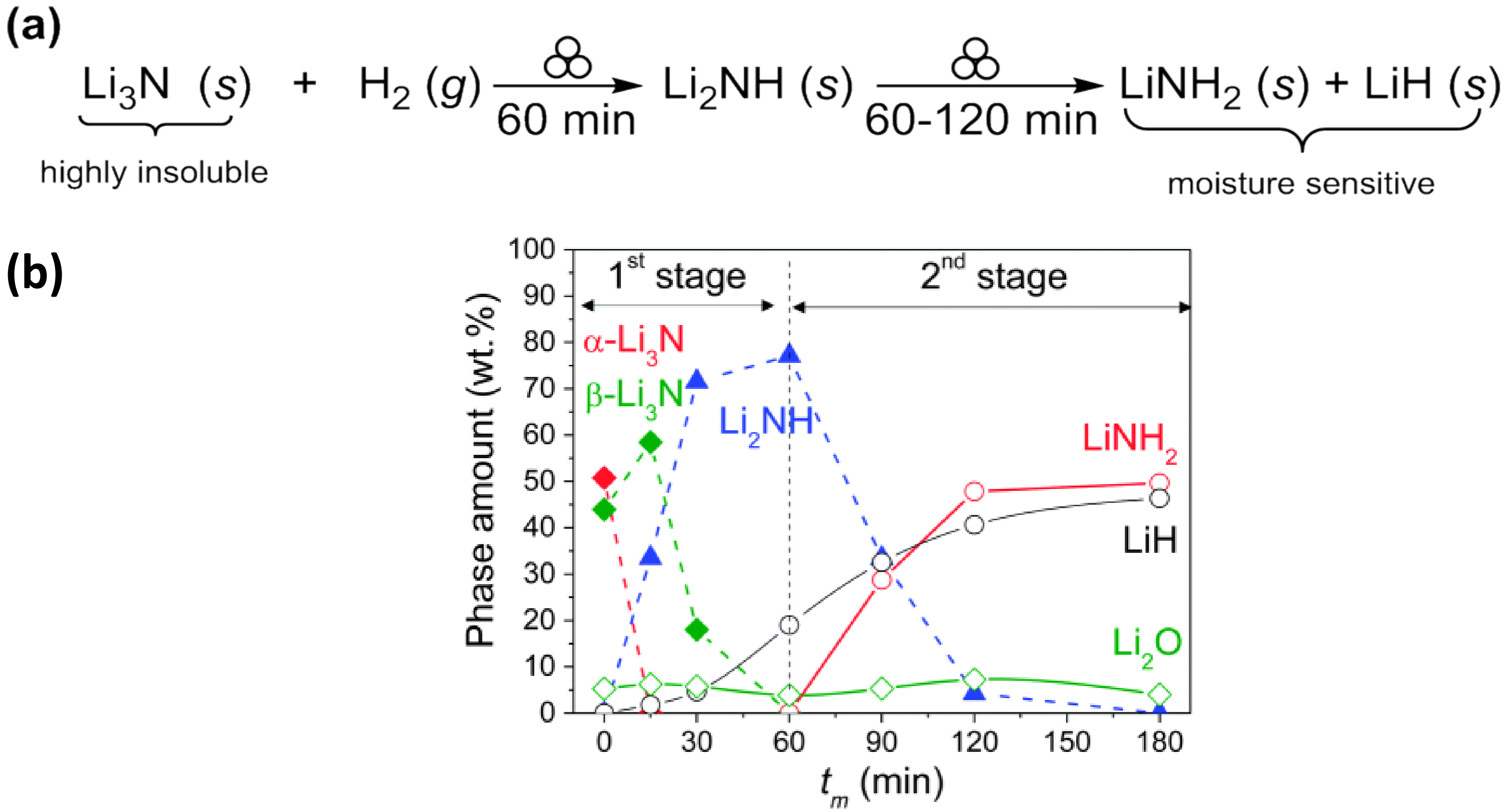

Figure 11. (a) Solid-gas reaction for the step-wise mechanochemical reduction of Li_3N by H_2. (b) Evolution of phase amounts during ball milling of Li_3N powder under hydrogen gas. Reproduced with permission from reference 29.

2.2 Materials containing s-block elementsecular species of the s-block

2.2.1 Group 1: Hydrides and alkaline metals

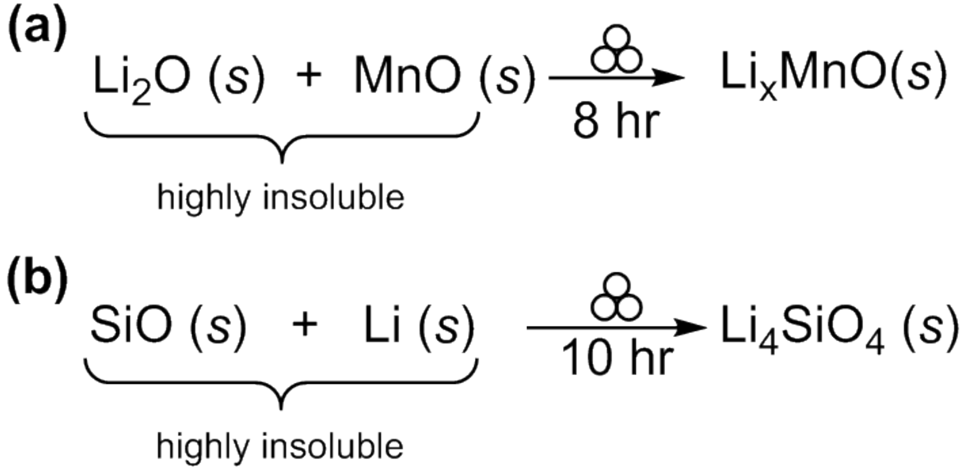

Scheme 5. (a) Synthesis of Li_xMnO spinels for ion batteries. (b) Synthesis of composite Li_4SiO_4 materials for lithium ion-batteries.

2.2 Materials containing s-block elementsecular species of the s-block

2.2.2 Group 2: alkaline-earth metals

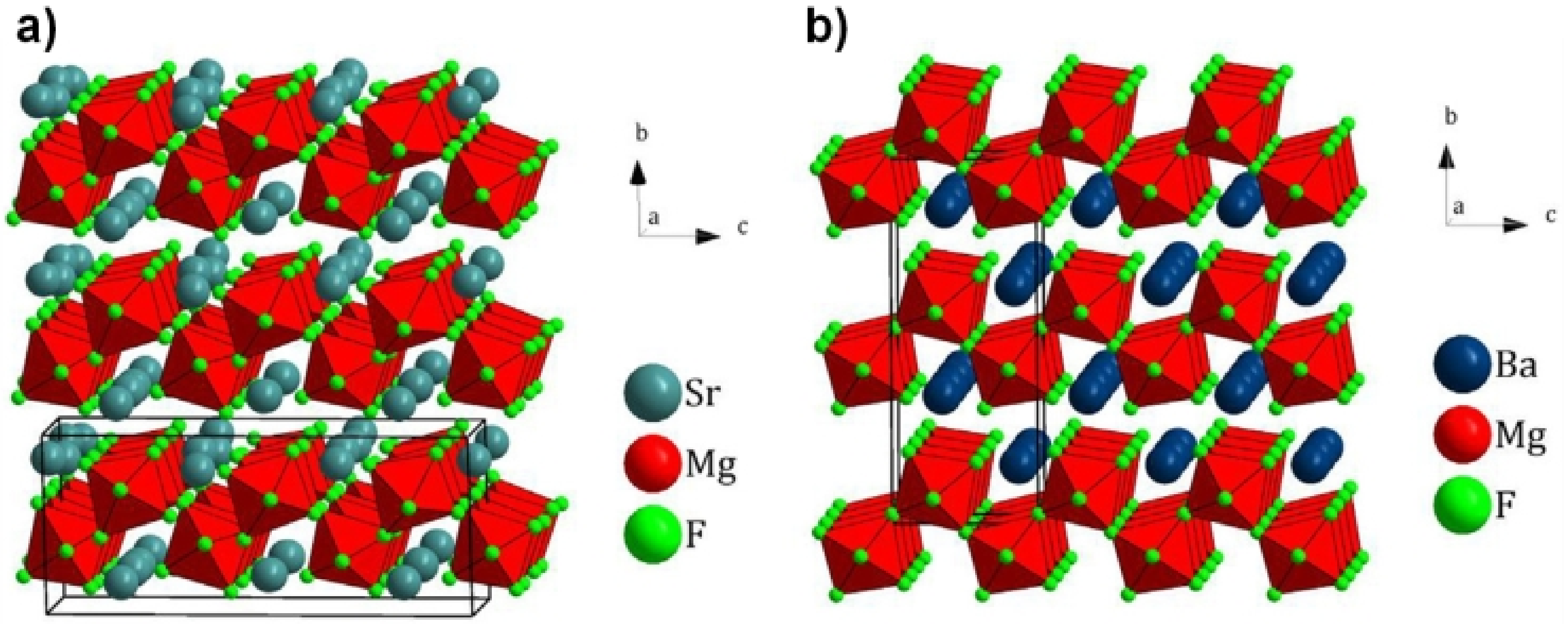

Figure 12. Crystal structures of (a) $SrMgF_4$, (P_{21}) and (b) $BaMgF_4$, (Cmc21). Unit cells are indicated by black lines. Mg is in the middle of the red octahedra. Reproduced with permission from reference 33

3. p-block compounds: from the “air-sensitive” boron, carbon and pnictogen groups, to stable chalcogens and halogens.

3.1 Molecular synthesis and transformations

3.1.1 Group 13: the boron group

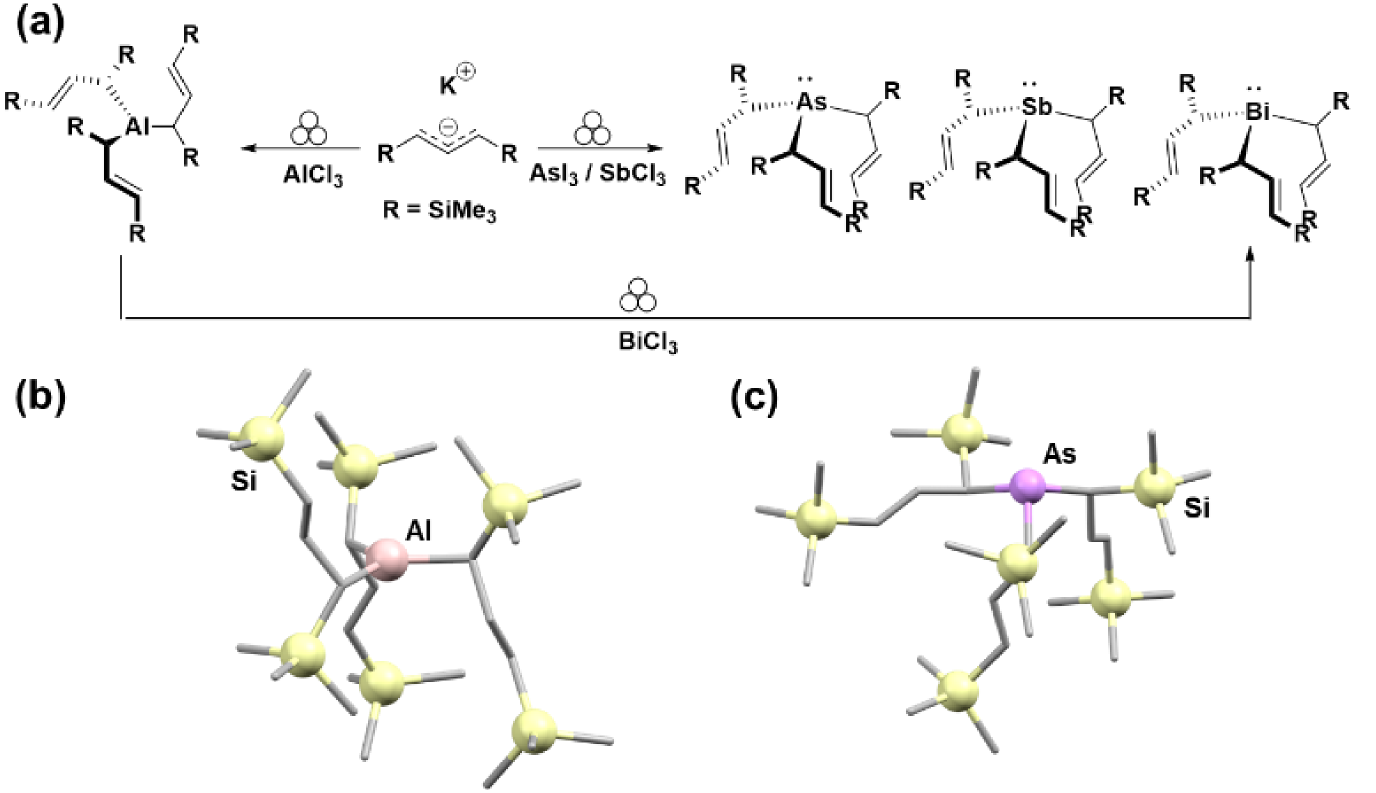

Figure 13. (a) Mechanochemical formation of the coordinatively unsaturated aluminium-, arsenic-, antimony- and bismuth-tris(trimethylsilyl)propyl complexes (for groups 15 compounds *vide infra*). Molecular structures of the (b) aluminium- and (c) arsenic tris(trimethylsilyl)propyl organometallic complexes as determined by X-ray diffraction crystallography. Hydrogen atoms are omitted for clarity.

3.1 Molecular synthesis and transformations

3.1.1 Group 13: the boron group

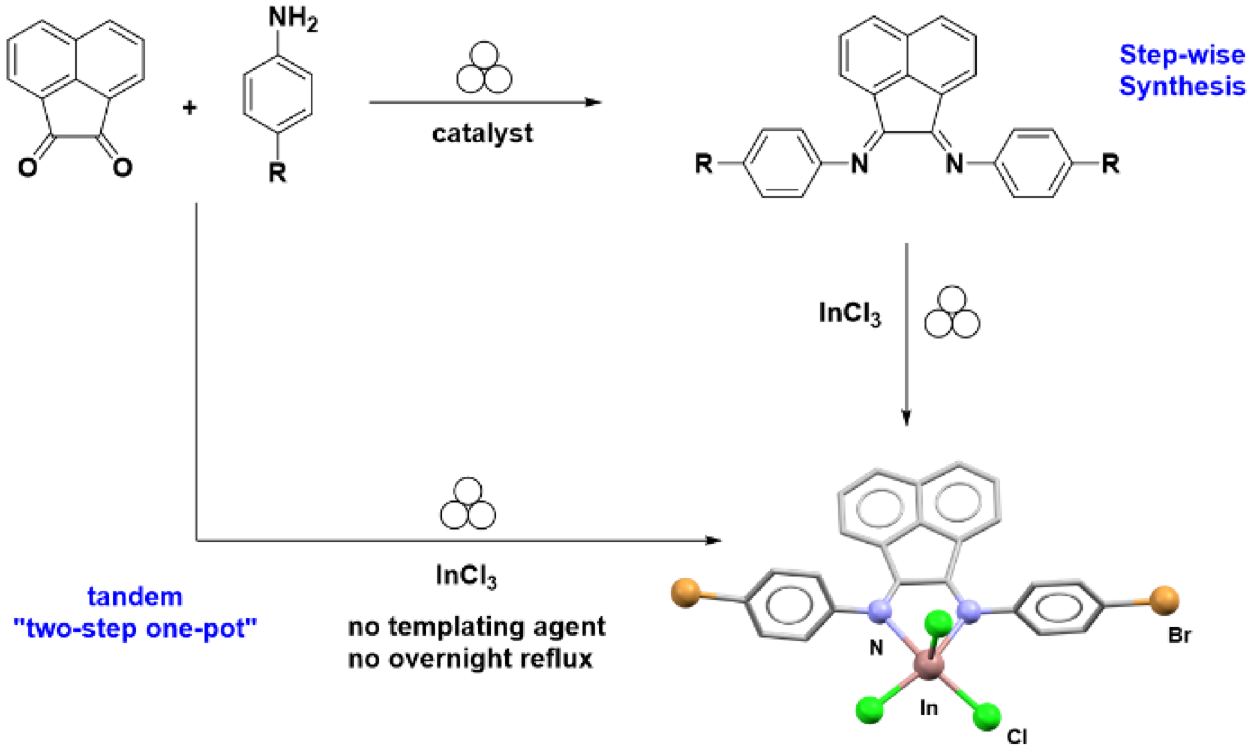

Figure 14. Tandem two-step one-pot mechanochemical formation of In-BIAN complex with molecular structure of the product, as determined by X-ray diffraction crystallography. Hydrogen atoms are omitted for clarity.

3.1 Molecular synthesis and transformations

3.1.2 Group 14: the carbon group

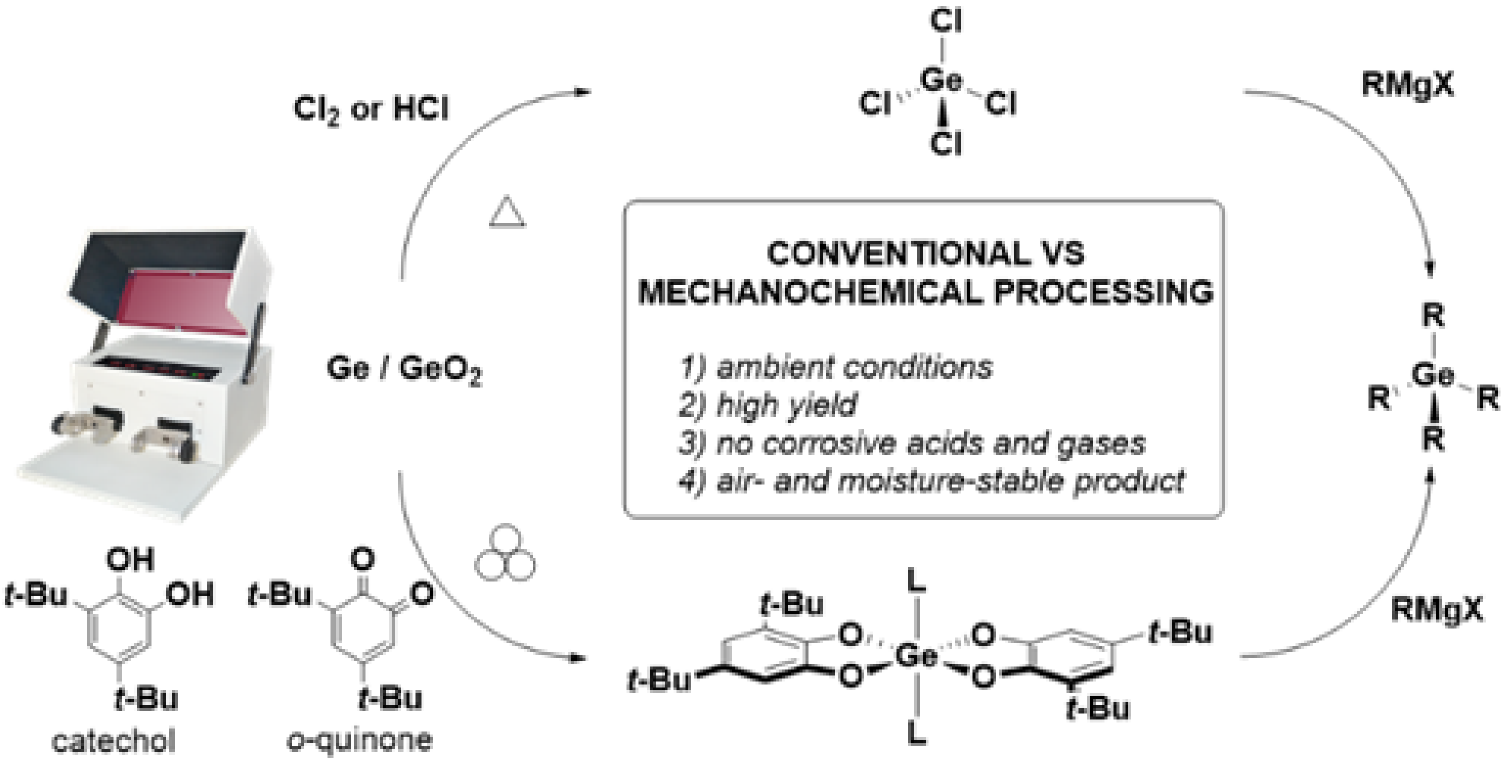

Scheme 6. Comparison of the mechanochemical and solution methods to achieve organo-germane compounds.

3.1 Molecular synthesis and transformations

3.1.2 Group 14: the carbon group

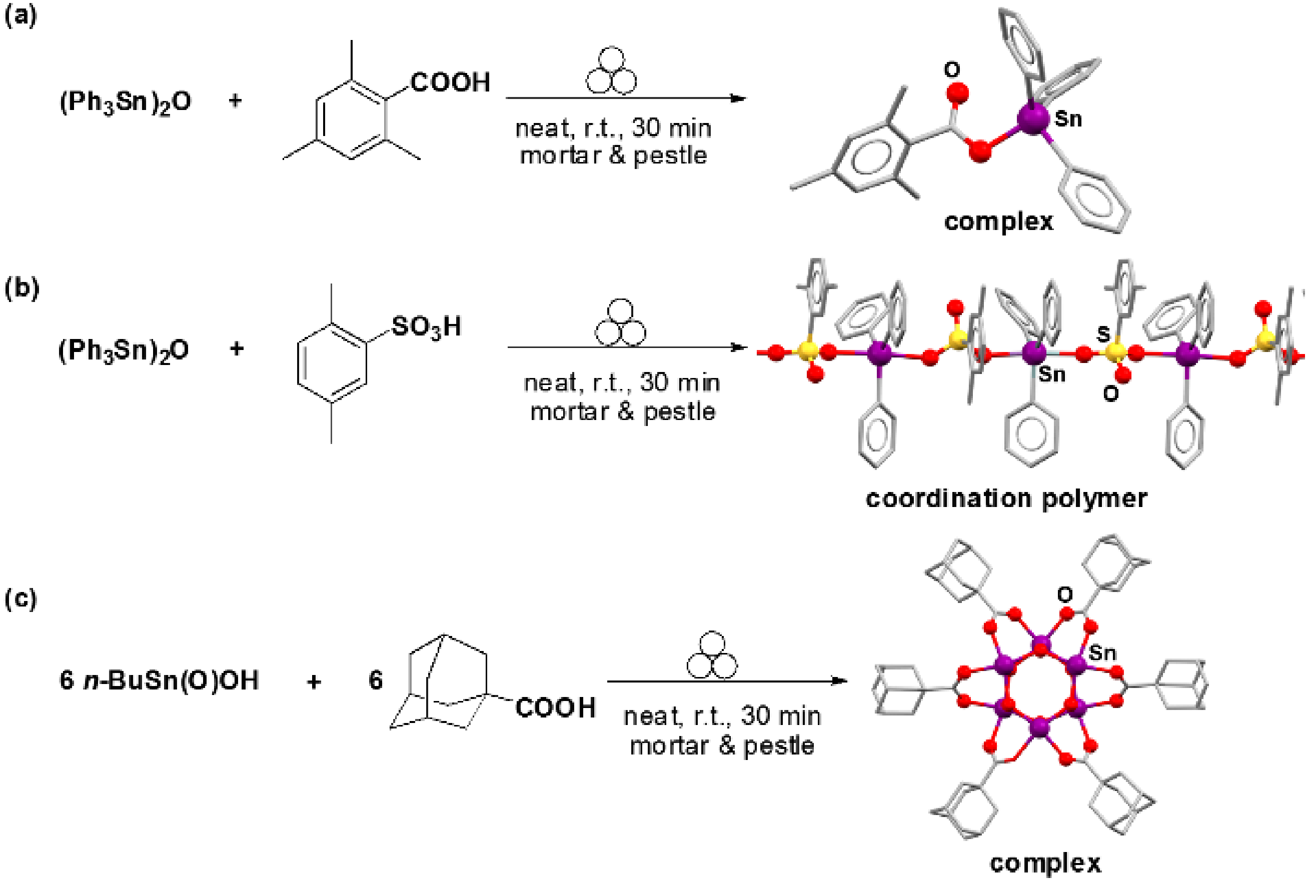

Figure 15. Formation of (a) molecular complex and (b) 1D coordination polymer by grinding $(Ph_3Sn)_2O$ with different organic acids in a mortar and pestle. (c) Formation of a hexameric Sn-cluster using polymeric organo-tin precursors and adamantyl-carboxylic acid. Hydrogen atoms are omitted for clarity.

3.1 Molecular synthesis and transformations

3.1.3 Group 15: pnictogens

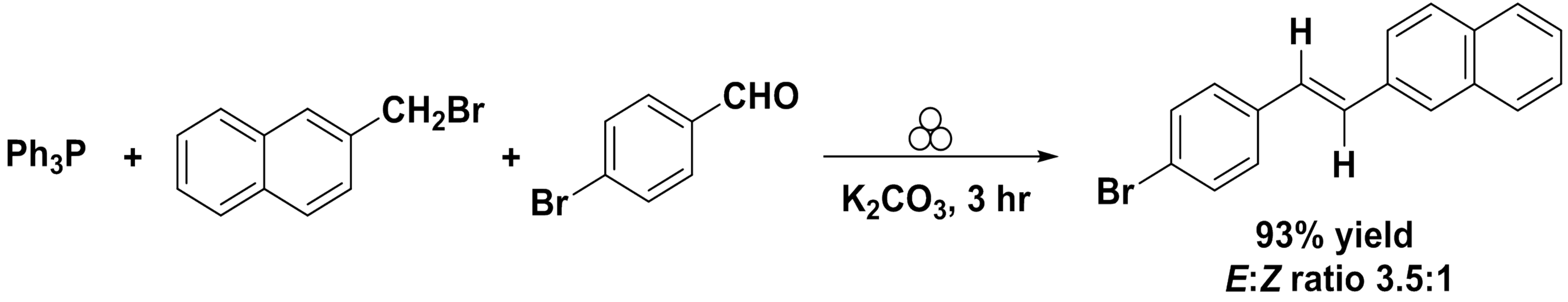

Scheme 7. One-pot Wittig reaction *via in-situ* formation of the phosphorus ylide by mechanochemistry as reported by Pecharsky.

3.1 Molecular synthesis and transformations

3.1.3 Group 15: pnictogens

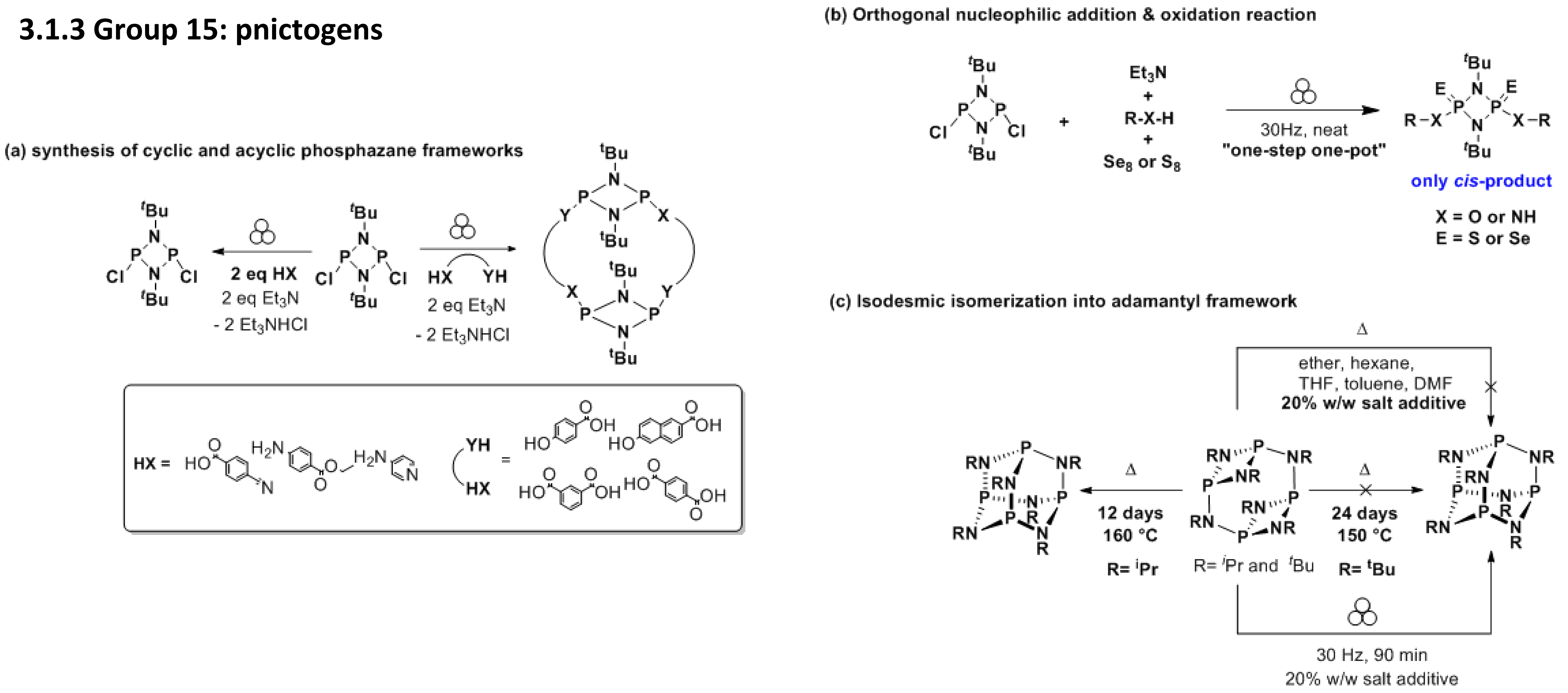

Scheme 8. (a) Mechanochemical synthesis of cyclic and acyclic phosphazane frameworks. (b) Orthogonal nucleophilic substitution and chalcogenic oxidation of cyclodiphosph(III)azanes. (c) Isodesmic rearrangement of the *tert*-butyl macrocyclic bis-cyclodiphosphazane into its adamantoid structure, enabled only by ball milling.

3.1 Molecular synthesis and transformations

3.1.4 Group 17: halogens

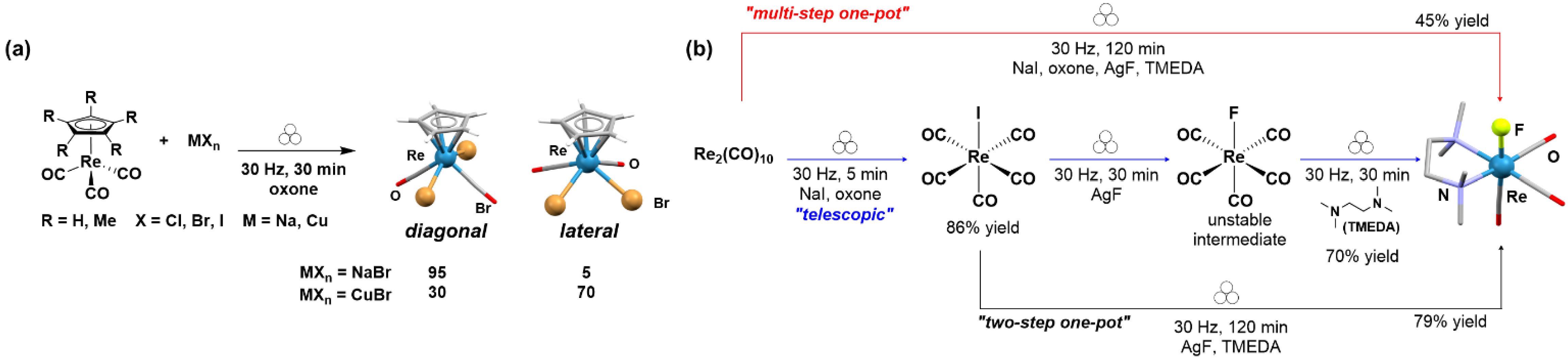

Figure 16. (a) Mechanochemical bromination of organometallic rhenium complexes using oxone and NaBr or CuBr.[45] (b) Multistep mechanochemical transformation of $Re_2(CO)_{10}$ to mono-rhenium complexes. Hydrogen atoms are omitted for clarity.[46]

3.2 Materials containing p-block elements

3.2.1 Group 13

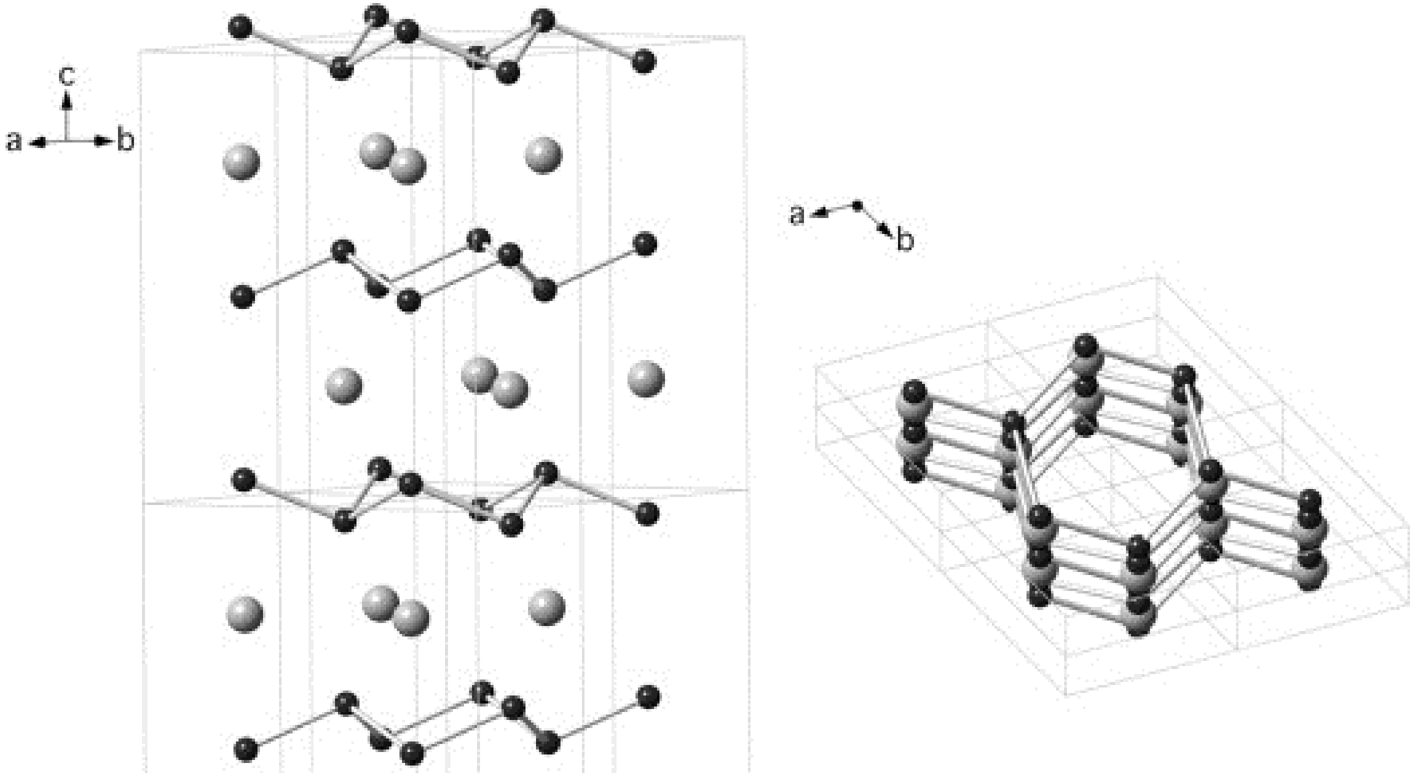

Figure 17. Crystal structure of hexagonal OsB_2. Osmium atoms are the larger gray spheres, and boron atoms are the smaller black spheres. Reproduced with permission from reference 47.

3.2 Materials containing p-block elements

3.2.1 Group 13

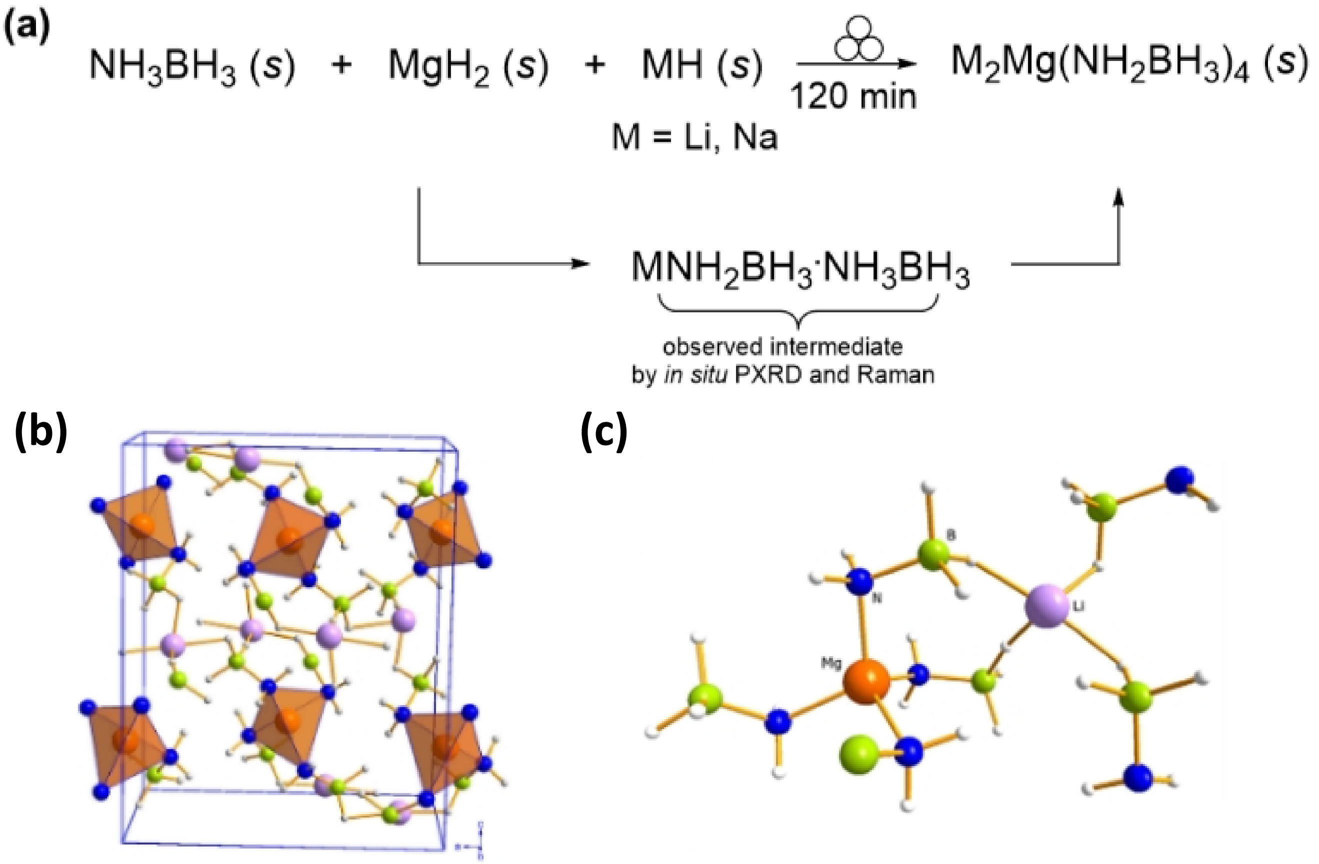

Figure 18. (a) Mechanochemical formation of mixed metal amido-boranes. (b) Crystal packing and (c) bonding environment of DLMAB. Each Mg^{2+} is bound to four N− forming a tetrahedron with $NH_2BH_3^-$ groups, and each Li^+ is octahedrally coordinated through six hydride H atoms of $NH_2BH_3^-$ moieties. Reproduced with permission from reference 48.

3.2 Materials containing p-block elements

3.2.2 Group 14: the carbon group

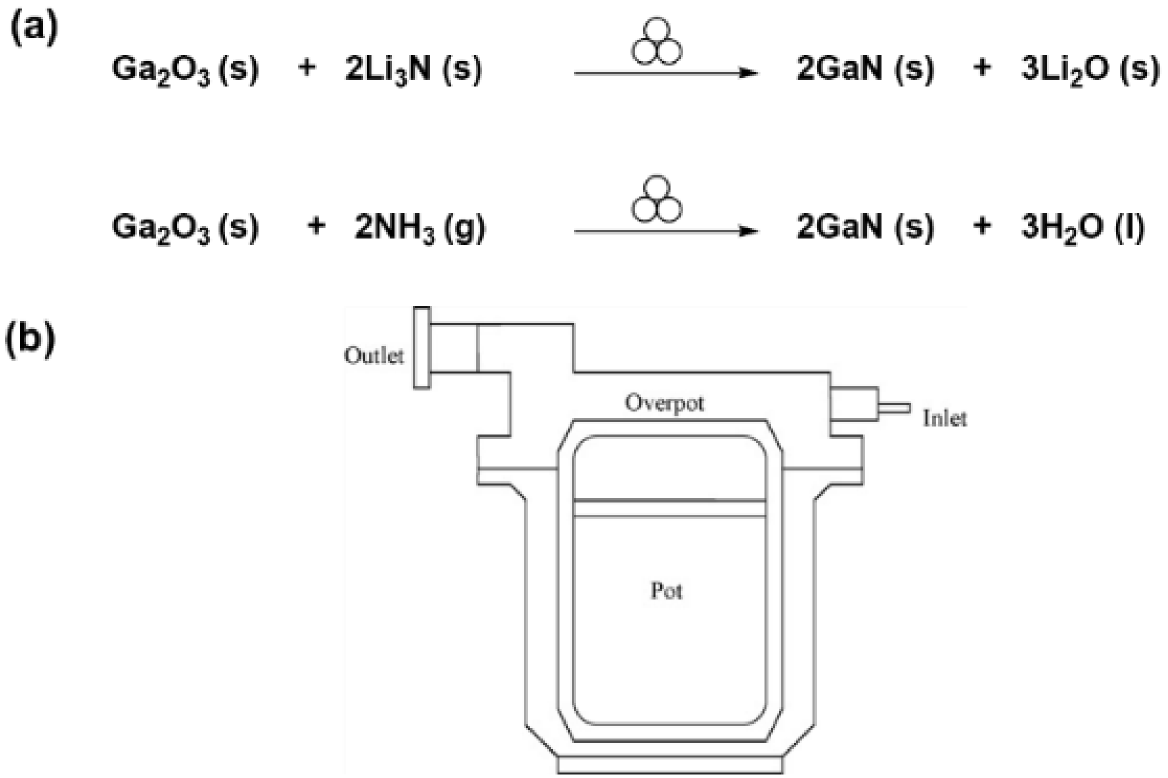

$$Ga_2O_3\,(s) + 2Li_3N\,(s) \longrightarrow 2GaN\,(s) + 3Li_2O\,(s)$$

$$Ga_2O_3\,(s) + 2NH_3\,(g) \longrightarrow 2GaN\,(s) + 3H_2O\,(l)$$

Scheme 9. (a) Mechanochemical reaction between Ga_2O_3 with Li_3N and NH_3, to form GaN. (b) Illustration of ZrO_2 reactor with Ga_2O_3 and Li_3N sample mixture within the overpot and gas flow arrangement. Reproduced with permission from reference 49.

3.2 Materials containing p-block elements

3.2.2 Group 14: the carbon group

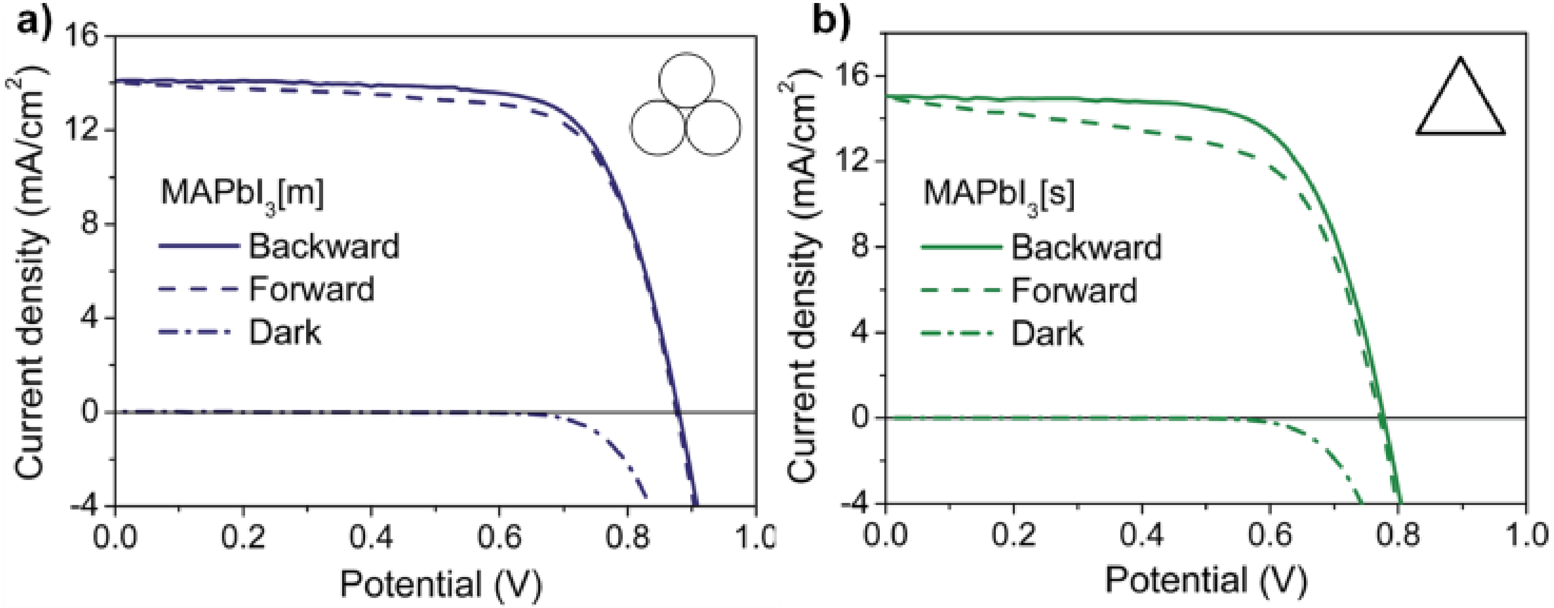

Figure 19. Current–voltage measurements of the MAPbI$_3$ perovskite devices prepared synthesized (a) mechanochemically and (b) by solution methods, to compare the hysteresis effect. Reproduced with permission from reference 50.

3.2 Materials containing p-block elements

3.2.2 Group 14: the carbon group

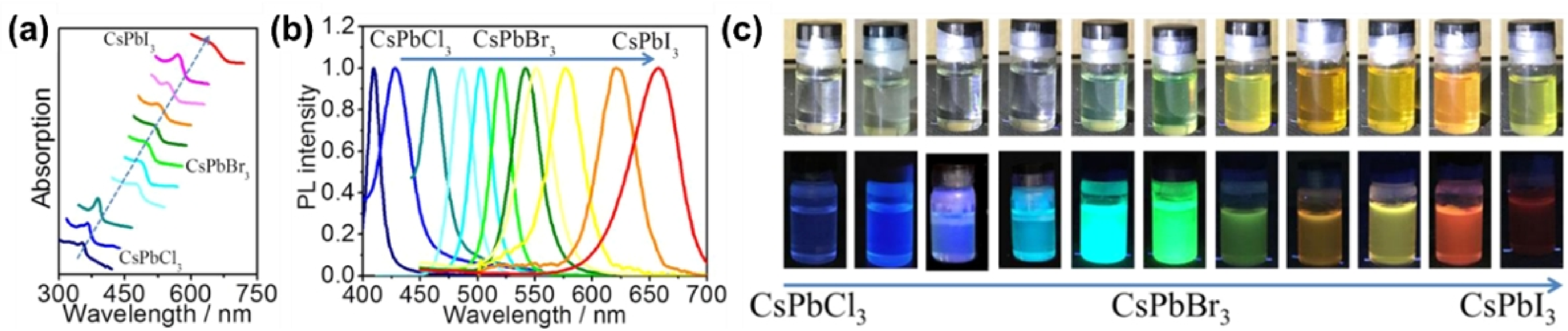

Figure 20. (a) Stacked UV−vis absorption spectra and (b) normalized fluorescence spectra of the mechanosynthesized CsPbX$_3$. (c) QDs with varying halide ratios. Reproduced with permission from reference 52.

3.2 Materials containing p-block elements

3.2.3 Group 15: the pnictogens

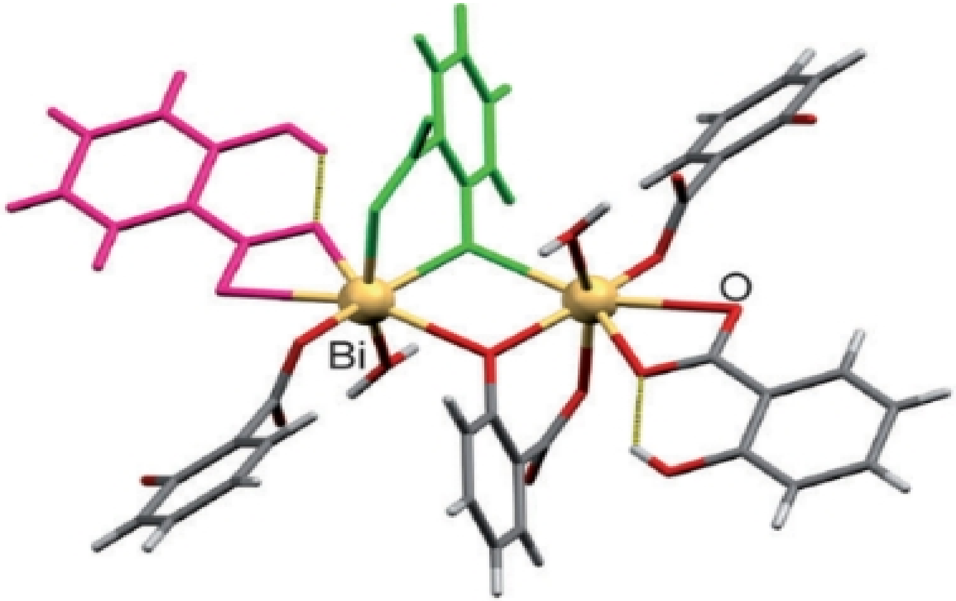

Figure 21. Fragment of a bismuth disalicylate sheet highlighting different bonding modes of doubly deprotonated sal (green) and singly deprotonated Hsal (purple) anions. Reproduced with permission from reference 53.

3.2 Materials containing p-block elements

3.2.3 Group 15: the pnictogens

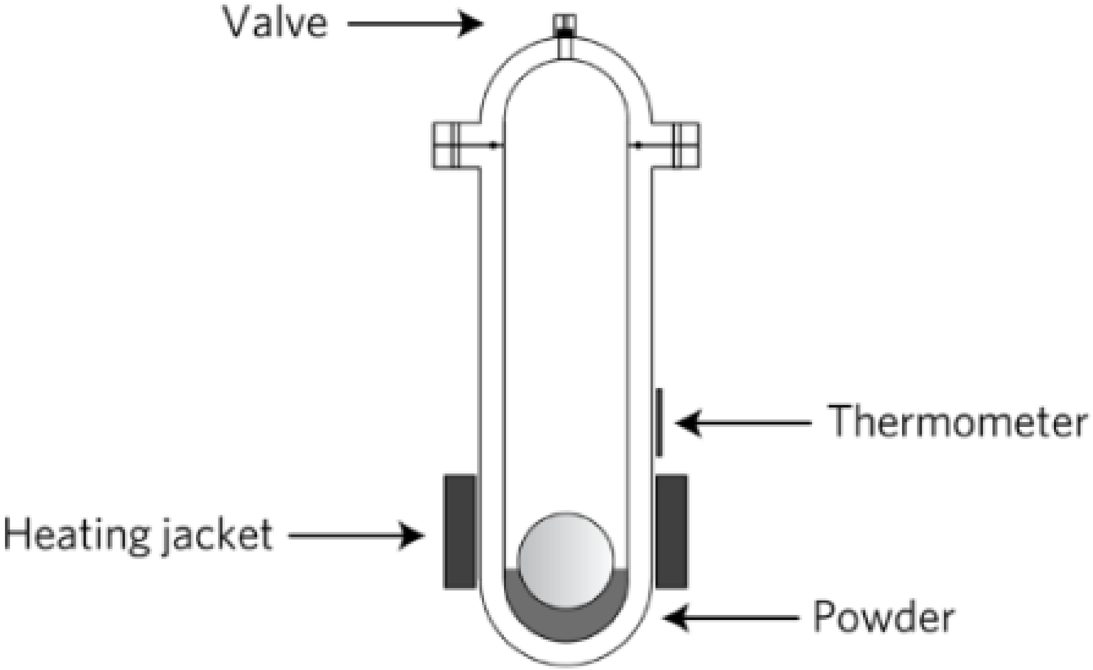

Figure 22. Diagram depicting the ball drop reactor for the impact force induced formation of Bi_2Te_3. Reproduced with permission from reference 54.

3.2 Materials containing p-block elements

3.2.4 Group 16: chalcogens

Figure 23. Pictures of the eccentric vibratory mill with attached closed satellite and open satellite filled with balls. Reproduced with permission from reference 56.

.

4. Synthesis of Nanoparticles containing Main Group Elements.

4.1 Top-down approach to nanoparticles

3.2.2 Group 14: the carbon group

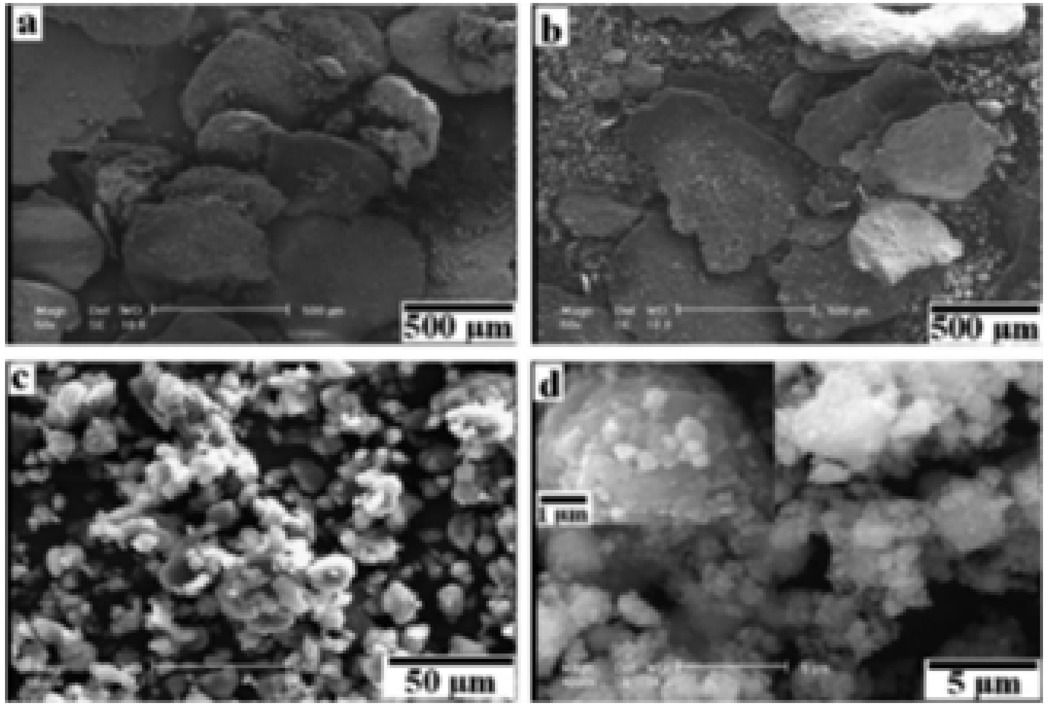

Figure 24. SEM images of the powders after (a) 2 hrs, (b) 20 hrs (c) 60 hrs and (d) 80 hrs of milling times, for the reaction between Mg, C and B_2O_3 to form B_4C. Reproduced with permission from reference 57.

4.1 Top-down approach to nanoparticles

4.2 Bottom-up approach to nanoparticles

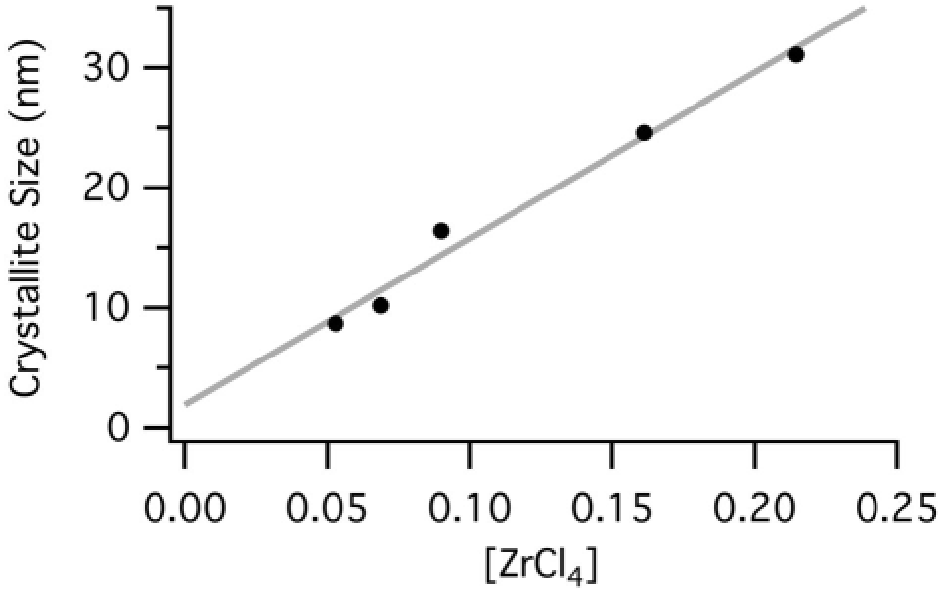

Figure 25. Correlation between the particle size and the effective concentration of $ZrCl_4$, as expressed in terms of moles per litre of free volume 58.